MÉTODOS NUMÉRICOS EN INGENIERÍA V
J. M. Goicolea, C. Mota Soares, M. Pastor y G. Bugeda (Eds.)

CONCRETE BEAMS REINFORCED WITH CARBON LAMINATE STRIPS BONDED INTO SLITS

Joaquim Barros, Adriano Fortes

- Departamento de Engenharia Civil
- Escola de Engenharia da Universidade do Minho
- Azurém, 4800 Guimarães, Portugal

e-mail: barros@eng.uminho.pt

Palabras clave: Carbon fibre reinforced polymer, epoxy adhesive, strengthening, finite element method, material non-linear analysis, tension stiffening, smeared crack

Resumen: *A strengthening technique based on carbon laminate (CFRP) strips applied into slits cut on the concrete cover, and bonded to concrete by epoxy adhesive, was used for increasing the load bearing capacity of concrete beams failed by bending. This technique avoids the occurrence of the peeling phenomenon, mobilizes high percentage of the full strengthening capacity of the CFRP used, and provides higher protection against fire and vandalism. The adopted strengthening technique is briefly described and the main results obtained are presented and discussed. Using a numerical model developed for non-linear analysis of reinforced concrete structures, the response of the beams tested was predicted. The applicability of this kind of models in such type of reinforced concrete structures is commented.*

1. INTRODUCTION

Due to the high strength-to-weight and stiffness-to-weight ratios, corrosion resistance, lightness, high durability and easy application, carbon fibre reinforced polymer products (CFRP) have being replacing steel systems and concrete jackets on structural strengthening and retrofitting [1].

Current strengthening techniques are based on gluing laminates or sheets of carbon fibre reinforced polymer onto the surface of the element to be strengthened. Due to peeling phenomenon [2] it is current to attain 40% to 70% of the tensile strength of these composites [1-3].

Since 1999 a different strengthening technique has being investigated in the Laboratory of the Civil Department, at Minho University. This technique is based on bonding strips of carbon fibres reinforced polymer laminates (with a cross section of $\approx 9.5 \times 1.5$ mm^2) into slits cut in the concrete cover of the beam surface to be submitted to tensile stresses. Four sets of beams reinforced with different percentage of conventional longitudinal steel bars were tested. Each series was composed by two beams, one strengthened with an amount of CFRP laminates for doubling the ultimate load of the other beam, not strengthened, designated in the present work by reference beam. The main results obtained are included in the present work.

Since all the intervening materials were tested, the data necessary for performing the numerical simulation of the behaviour of the beams tested was available. An important point was to verify if the tension-stiffening model, implemented into the computational code developed for concrete reinforced with conventional bars and/or discrete fibres [4], was appropriated for this kind of structures, where a strip of CFRP was considered perfectly bonded to concrete up to its rupture. The numerical simulations performed are presented and analysed.

2. EXPERIMENTAL WORK

2.1 Characterization of the materials

The concrete was manufactured in the laboratory, a commercial supplier has furnished the steel bars, BETTOR MBT® Portugal has given the CFRP laminates and the adhesives.

2.1.1 - Concrete

The compression strength of the concrete used was determined from uniaxial compression tests carried out with cylinders of 150mm diameter and 300mm height. From the ten tests it was obtained an average compression strength of 46.1MPa, with a standard deviation of 2.6MPa and a coefficient of variation of 5.7%.

2.1.2 – Steel bars

In beams it was applied longitudinal bars of 6 mm and 8 mm diameter. The stirrups were made by steel bars of 6 mm diameter and wires of 3 mm diameter. The stress-strain relationships for the ϕ6 and ϕ8 steel bars are depicted in Figure 1, and were obtained from uniaxial tests carried out in a servo-controlled load frame.

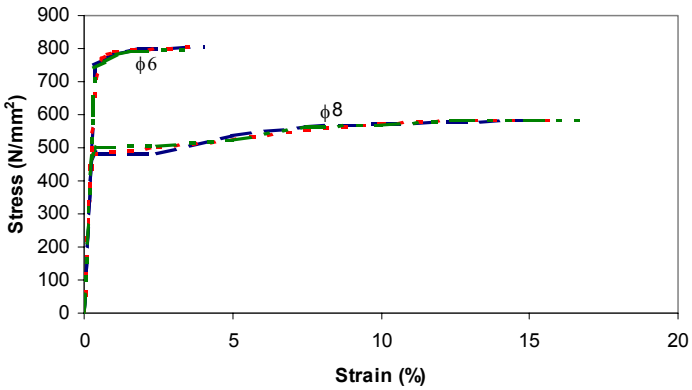

Figure 1. Stress-strain relationship of the longitudinal bars applied in the beams.

2.1.3 – Laminates of CFRP

The CFRP laminates were provided in rolls, produced by S&P® and distributed by Bettor MBT® Portugal, and have a cross section of 9.5 mm width and 1.5 mm thickness. To evaluate the corresponding tensile strength and Young modulus, uniaxial tensile tests were carried out in a servo-controlled test machine (Instron, series 4208), according to the recommendations of ISO 527-5:1997 [5]. From these tests a Young modulus of 158 GPa and a tensile strength of 2700 MPa were obtained.

2.1.4 – Adhesives

An epoxy adhesive, furnished by Bettor MBT® Portugal, was used to bond the CFRP laminates to the concrete. From uniaxial tensile tests carried out according to the recommendations of ISO 527-3:1997 [6] it was evaluated a Young modulus of 5.0 GPa and a tensile strength ranged from 16 MPa up to 22 MPa.

2.2 - Beams

Figure 2 represents the geometry of the beams, the reinforcement arrangement and the number and position of the CFRP laminates. The loading and the support conditions are also schematised. The cross section area of the CFRP laminates (A_L) applied in the beam of each series was estimated in order to double the ultimate load of the corresponding reference beam. To perform this task it was used a cross section layer model described elsewhere [7]. The

number of CFRP laminates was the necessary for obtaining a cross section area as nearest as possible to the values determined from the numerical analysis. It was applied a percentage of stirrups for assuring bending failure modes, even for the beams strengthened. The length of the CFRP laminates was determined in order to have the embedded length necessary for sustaining the tensile stresses on the CFRP, installed at by the ultimate load, without occurring slip between CFRP laminates and surrounding concrete. To accomplish this task it was used the results obtained by Sena Cruz *et al.* [8] and Sena Cruz e Barros [9]. In Figure 2, A_s is the cross section area of the tensile longitudinal steel bars.

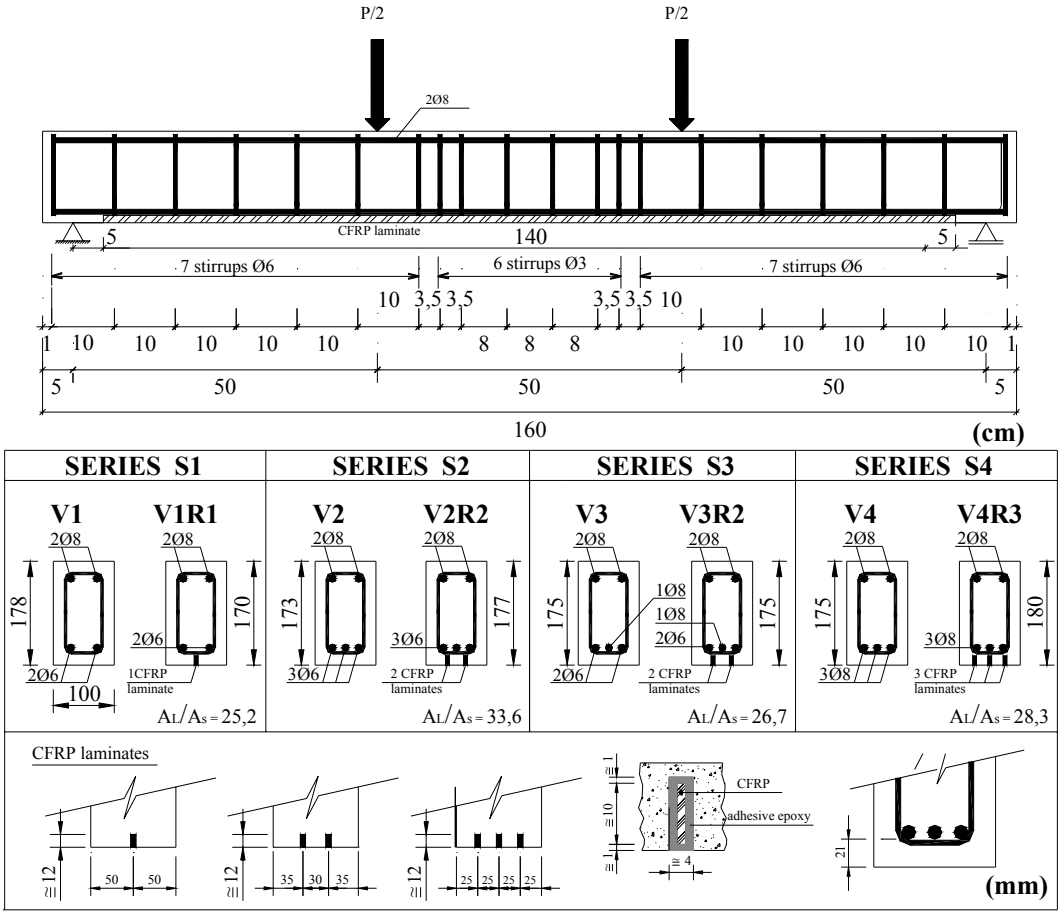

Figure 2. Series of beams tested.

2.3 - Strengthening technique

The strengthening technique in composed by the following procedures:

- Using a Hilti diamond cutter, model DC 230-S, it was executed slits of about 4.5 mm width and 12 mm depth on the concrete cover of the surface beam that will be in tension;
- The slits were cleaned by compressed air;

- The CFRP laminates were cleaned using acetone;
- Manufacture of the adhesive according to the supplier instructions;
- Fill the slits with the adhesive;
- Application of the adhesive on the faces of the CFRP laminates;
- Introduce the CFRP laminates into the slits.

Figure 3 illustrates the procedure of sawing the slits and Figure 4 shows the aspect of the slits after have being sawed. At least five days were spent on the curing/hardening process of the epoxy adhesive, before testing the corresponding beam.

Figure 3. Sawing the slits.

Figure 4. Final aspect of the slits.

2.4 - Test set up and equipment

Figure 5 is a representation of the reaction frame, actuator and load cell used on the tests. Figure 6 illustrates the disposition of the LVDTs supported in a Japanese Yok system [10] (for avoiding the register of extraneous displacements) and the place and the reference of the strain gauges applied on a lateral surface of the CFRP laminates. The tests were carried out under the displacement control of the LVDT placed at mid-span, using a displacement ratio of 20μm/s.

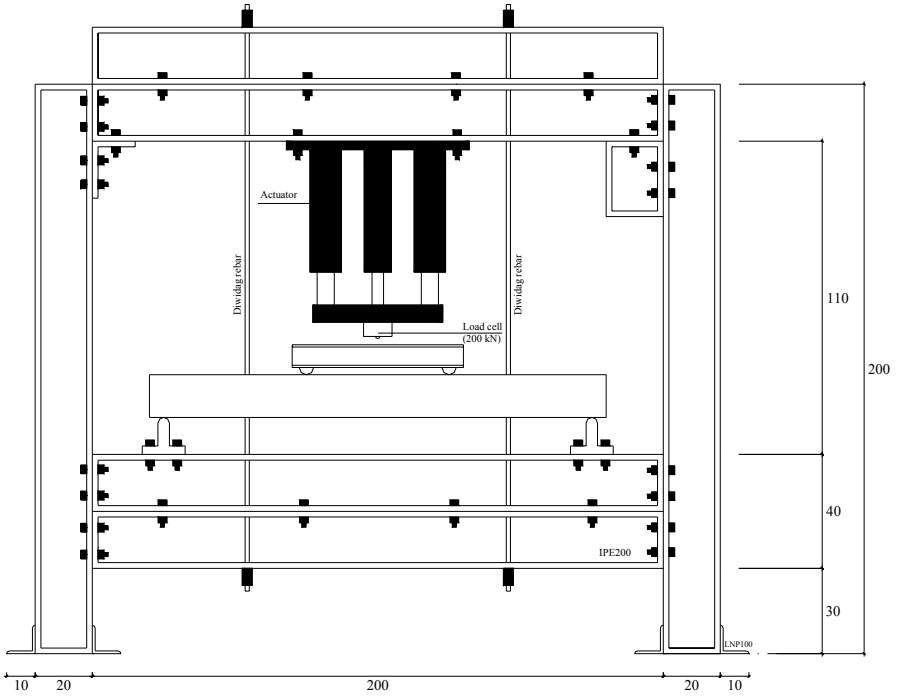

Figure 5. Test set-up.

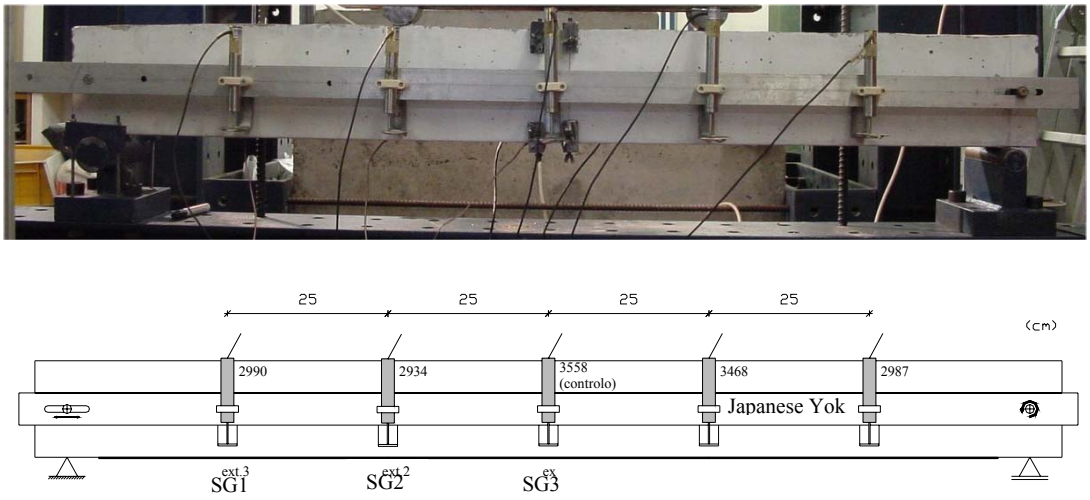

Figure 6. Displacement transducers and strain gauges applied.

2.5 - Failure modes

Figure 7 includes photos of the beams tested, after failed. In the reference beams it was developed, basically, flexural cracks. The longitudinal steel bars have yielded and the tests were interrupted when the deflection at mid span was higher than 20 mm. Therefore, the failure mode of the reference beams was ductile, by bending.

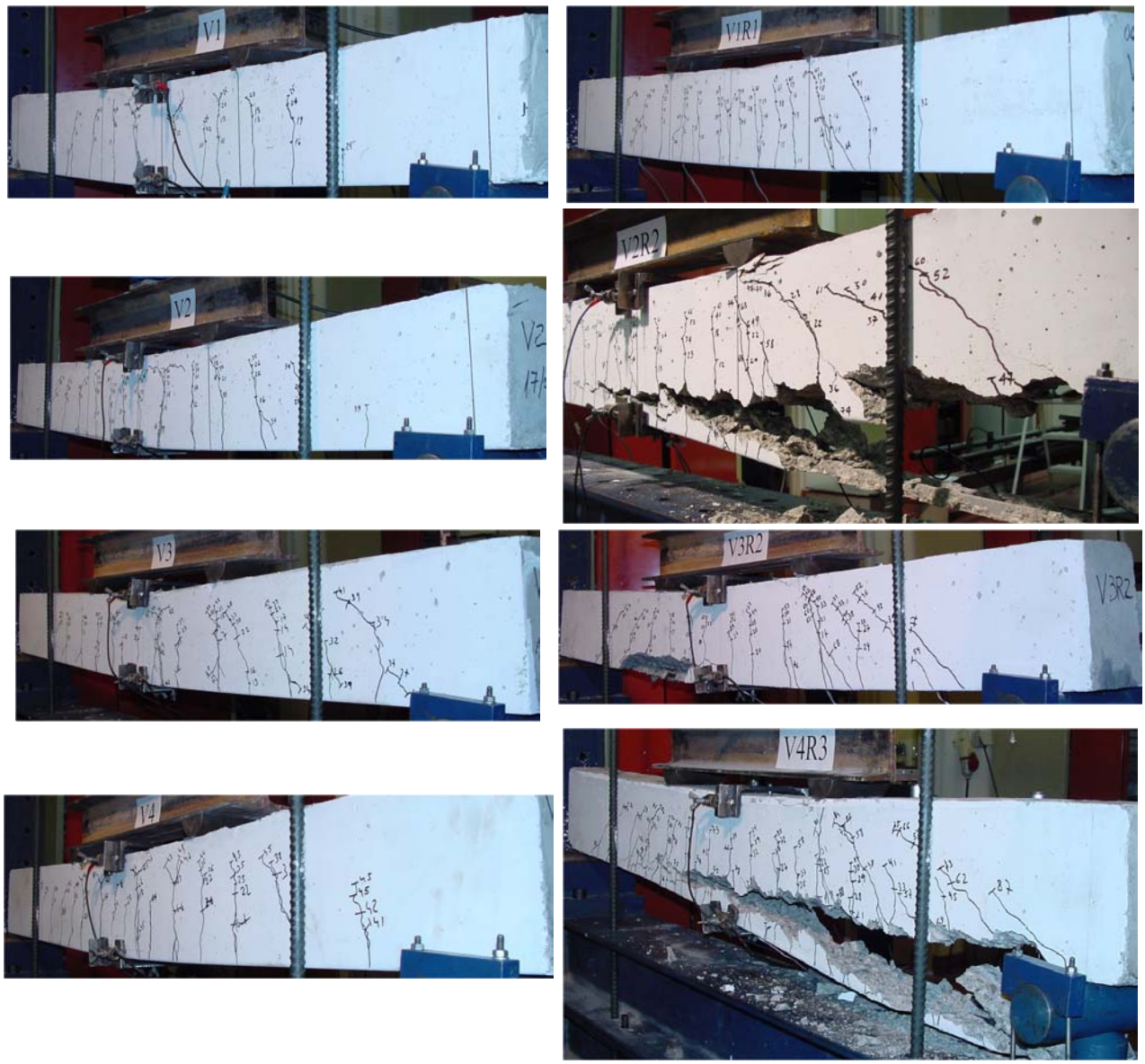

(a) (b)

Figure 7. Aspect of the beams at the end of the tests: (a) Reference beams; (b) Strengthened beams.

In strengthened beams, apart beam V1R1, the remainder have failed by the detachment of a concrete layer at bottom beam surface. This layer had non-homogeneous thickness, and attained 60 mm in some parts, which reveals that, not only the concrete cover was detached, but also parts of concrete above the longitudinal reinforcement. The test of beam V1R1 was interrupted when the deflection at mid-span was about 27 mm. For this deflection the beam had, basically, flexural cracks.

The tensile stresses in CFRP laminates are transferred to the surrounded concrete by shear stresses. The resultant of these shear stresses is applied near the geometric centre of the cross section of CFRP laminates, that is eccentric to the concrete weak surface (near the longitudinal steel bars), see Figures 7 and 8. This force induces shear and tensile stresses at this weak surface, decreasing the concrete strength at this micro-zone. Since this eccentricity is less than the one of current strengthening techniques (the laminates are glued on external surface), the decrease of the concrete strength of the weak zone is lesser, which is one justification for the higher efficacy of the strengthening technique proposed in the present work. Another mechanism supporting this higher performance resides on the fact that, in the present strengthening technique the laminate has both lateral faces glued to the concrete and are confined by the surrounded concrete, while in current strengthening techniques only one face of the CFRP is glued, and CFRP is not confined.

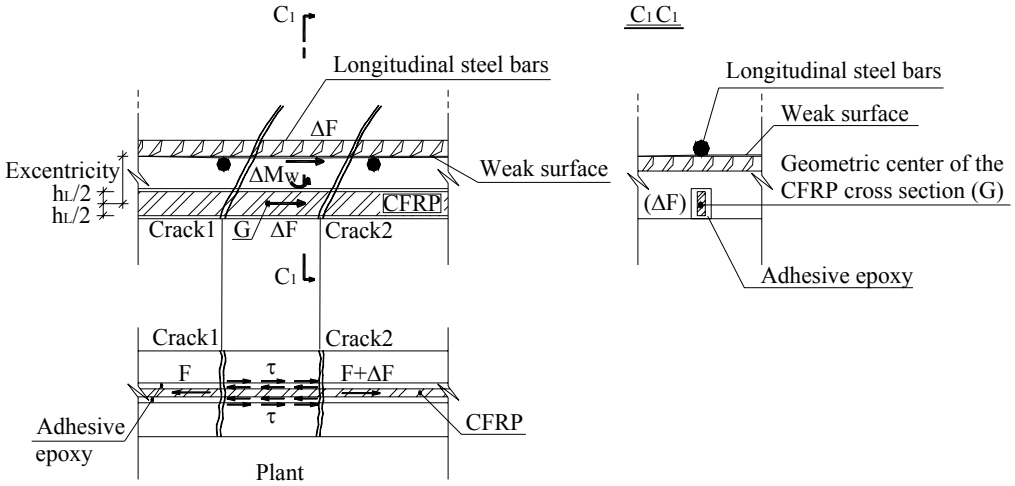

Figure 8. Failure micro-mechanisms.

2.6 - Results and comments

Table 1 includes the ultimate load and the ratio between the ultimate load of a strengthened beam and the ultimate load of its corresponding reference beam. Excluding series S1, where the test of the strengthened beam was interrupted at a load of 50.3kN when the deflection was about 27 mm, in the remainder series the purpose was attained, i.e., the strengthening strategy applied has practically doubled the ultimate load of the corresponding beams. Last column of Table 1 includes the strain at beam failure, measured in the strain gauge SG3 fixed to CFRP laminates (see Fig. 6). In general, the strain at failure is greater in beams with lower ratio A_L/A_s (see Figure 2). Dividing these maximum strain values by the ultimate strain of CFRP laminates (2700/158000=17.1‰) it was obtained values ranged from 62% up to 91% (see values in brackets), which denotes a good efficacy of the strengthening strategy proposed. Figure 9 shows the relationship between the force applied and the displacement measured at mid-span for the beams tested. From these relationships it can be observed that, up to the load at cracking, the rigidity of the reference and strengthened beams are practically the same.

After this point the increment on the rigidity is proportional to the ratio A_L/A_s . The presence of the CFRP laminates has increased the deflection corresponding to the moment when the steel bars have yielded. After this point (third branch) the rigidity of the strengthened beams has decreased, and the rigidity of this branch is higher for the beams with greater ratio A_L/A_s .

Series	Beam reference	P_{ult} (kN)	$(P_{ult})_{SB}/(P_{ult})_{RB}$ **	Strain*** (‰)
S1	V1	28.2	1.78	-
	V1R1	50.3*		15.5 [91]
S2	V2	41.0	1.91	-
	V2R2	78.5		12.8 [75]
S3	V3	41.3	1.98	-
	V3R2	81.9		12.8 [75]
S4	V4	48.5	1.96	-
	V4R3	94.9		10.6 [62]

* Test interrupted at a deflection of about 27mm; ** $(P_{ult})_{SB}$ - Strengthened beam; $(P_{ult})_{RB}$ - reference beam

*** Strain at beam failure, registered in strain gauge SG3 (see Fig. 6).

Table 1. Some results obtained.

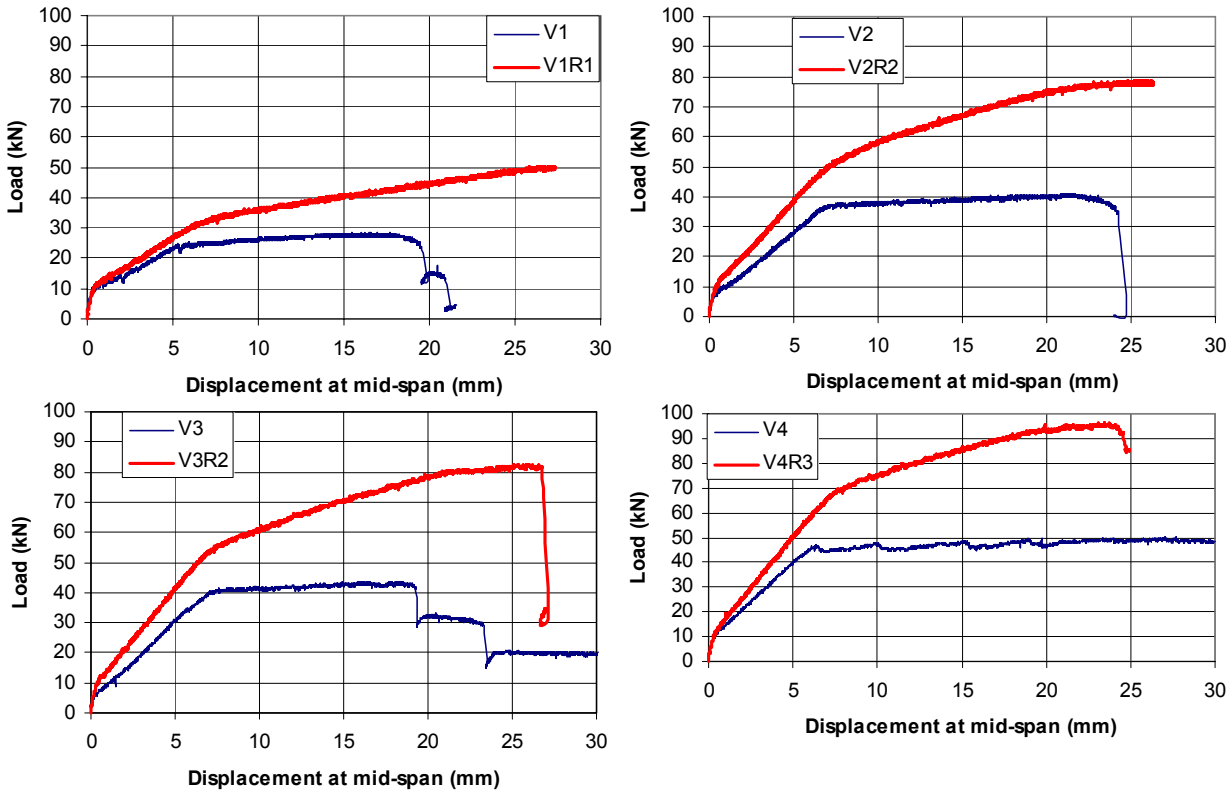

Figure 9. Force deflection relationship of the beams tested.

3 - NUMERICAL ANALYSIS

3.1 Brief description of the model

In the present model concrete cracking is simulated under the framework of the smeared crack concepts [4]. Non-orthogonal cracks can develop in a Gauss point of a finite element. According to the present model, the total strain increment in a cracked concrete element is the addition of the strain increment in the fracture zone (the width of the finite element over which the micro-cracks are smeared out) with the strain increment in concrete between cracks. The strain increment in the fracture zone is governed by the concrete fracture parameters [11], while the strain increment of the concrete between cracks is obtained using the theory of the elasto-plasticity applied to concrete [4]. The stress-plastic strain relationship used for defining the hardening modulus [12] was based on the stress-strain expression proposed by CEB-FIP Model Code 1990 [13]. Up to peak tensile strength it was assumed a linear elastic stress-strain relationship, governed by the concrete Young modulus and Poisson coefficient. After cracking, the fracture mode I for the concrete under the influence of reinforcing elements follows the tension-stiffening model schematically represented in Figure 10. The concrete fracture parameters and the characteristics of the reinforcing elements contribute for the shape of this diagram [4]. The relationship illustrated in Figure 11 governs the fracture mode I of the concrete that is not under the influence of the reinforcing elements. Values attributed to (ζ_1, α_1) and (ζ_2, α_2) define the shape of the tensile softening diagram. Its full characterization has the contribution of the concrete fracture energy (G_f) and the crack band width (l_b). The recommendations proposed by CEB-FIP Model Code 1993 were taken into account for defining the boundary between elements in softening and elements in stiffening.

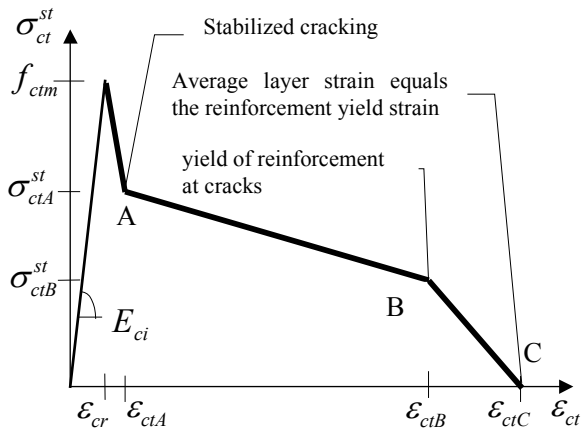

Figure 10. Tension stiffening diagram.

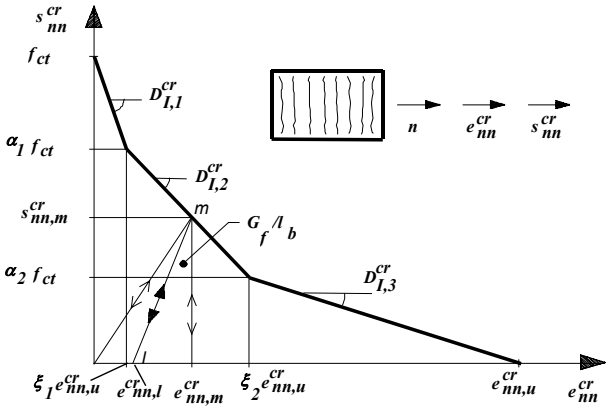

Figure 11. Trilinear tension softening diagram.

For simulating the decrease of the crack shear rigidity with the crack opening, the following expression was assumed for defining the parameter that affects the elastic shear modulus, G_c,

$$\beta = \left[1 - \frac{e_{nn}^{cr}}{e_{nn,u}^{cr}} \right]^{p} \quad (1)$$

where e_{nn}^{cr} is the crack strain normal to crack surface and $e_{nn,u}^{cr}$ is the ultimate normal crack strain. In the analyses carried out it was taken p=3. It was realized that, mainly for strengthened beams, decreasing the value of p parameter has lead to premature shear failures.

From the analysis performed it was observed that, the tension-stiffening model developed for concrete reinforced with conventional bars is not appropriate for concrete elements reinforced with bars and CFRP laminates, because steel bars and CFRP laminates have very different behaviour up to failure. A most appropriate model should be based on a diagram characterized by the following points: crack stabilization, yield of reinforcement at crack, average strain equals the reinforcement yield strain, failure of CFRP at crack, and average strain equals the failure strain of the CFRP. Since this model is not yet developed, the diagram indicated in Figure 11 was used, with some adjustments for taking into account the previous observations.

In the model developed, concrete elements can be reinforced with discrete or/and smeared steel bars, as well as strips of CFRP laminates. Not only the steel bars were considered perfectly bonded to concrete, but also CFRP laminates. This assumption is also reasonable for CFRP laminates because previous tests [8] have revealed that slip displacement is negligible if the embedded length of CFRP are greater than twenty times the equivalent diameter of its cross section ($\phi_{eq} = \sqrt{(4/\pi) \times A_L} = \sqrt{(4/\pi) \times 9.5 \times 1.5}$ =4.3 mm). The length of the CFRP laminates applied in beams was determined in order to assure an embedded length greater than the aforementioned value. Observing the aspect of the CFRP laminates after the failure of the strengthened beams, it was confirmed that these laminates were remained bonded to concrete.

3.2 Model application

Figure 12 represents the finite element mesh adopted on the numerical simulations. Due to symmetry conditions, only half beam was discretized in eight-nodded isoparametric plane stress elements. Two by two Gauss-Legendre integration points were used for evaluating the element stiffness matrix and the nodal forces equivalent to the internal stresses. The transversal and the longitudinal steel bars, as well as, the CFRP laminates, were all discretized in 1D bar element of 2 nodes, considered perfectly embedded into concrete. The first two rows of concrete elements were assumed under tension-stiffening, while the remainder elements were considered under tension-softening. In the analysis carried out, a new set of smeared crack can develop in a cracked concrete, only if the maximum principal stress has surpassed the concrete tensile strength and the angle between the new and previous cracks is higher than sixty degrees. Table 2 and 3 include the values of the materials

parameters adopted in the numerical simulation for the concrete and for reinforcing elements, respectively.

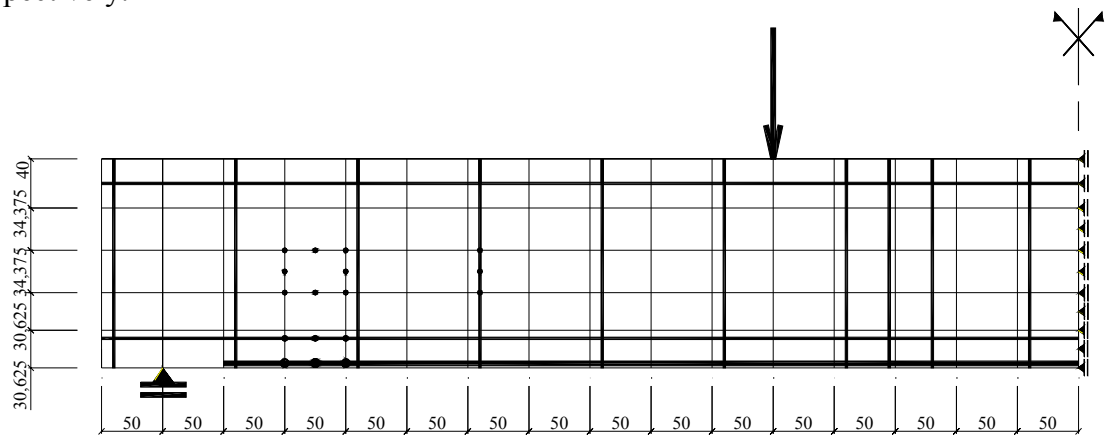

Figure 12. Finite element mesh (dimensions in mm).

CONCRETE
Compression strength = 46 MPa; Strain at peak compression stress = 2.2×10^{-3}; Tension strength = 3.0 MPa; Young Modulus = 35757 MPa; Poisson coefficient = 0.15; Crack band width = (finite element area)$^{1/2}$
Softening (same parameters for all beams) $G_f = 0.087\,\text{N/m};\ \alpha_1 = 1/3;\ \zeta_1 = 0.02;\ \alpha_2 = 1/6;\ \zeta_2 = 0.48$
"Stiffening" Reference beams (V1, V2, V3 and V4): $"G_f" = 0.24\,\text{N/m};\ \alpha_1 = 0.5;\ \zeta_1 = 0.05;\ \alpha_2 = 0.4;\ \zeta_2 = 0.8$ Strengthened beams (V1R1, V2R2, V3R2 and V4R3: $"G_f" = 0.7\,\text{N/m};\ \alpha_1 = 0.6;\ \zeta_1 = 0.1;\ \alpha_2 = 0.3;\ \zeta_2 = 0.45$

Table 2. Values for concrete properties.

REINFORCING ELEMENTS	
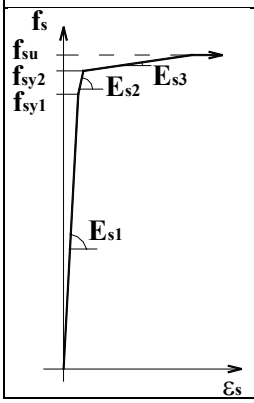	ϕ3 STEEL WIRES E_{s1}=195 GPa; f_{sy1}=175.0 MPa; E_{s2}=2 GPa; f_{sy2}=200.0 MPa; E_{s3}=2 GPa; f_{su}=288MPa
	ϕ6 STEEL BARS E_{s1}=200 GPa; f_{sy1}=700.0 MPa; E_{s2}=40 GPa; f_{sy2}=760.0 MPa; E_{s3}=1.5 GPa; f_{su}=800MPa
	ϕ8 STEEL BARS E_{s1}=200 GPa; f_{sy1}=473.0 MPa; E_{s2}=0.25 GPa; f_{sy2}=485.0 MPa; E_{s3}=4 GPa; f_{su}=582MPa
	CFRP LAMINATES E_{s1}= E_{s2}= E_{s3}=158000.0 MPa; f_{sy1}= f_{sy2}= f_{su}=2700 MPa

Table 3. Values for properties of reinforcing elements.

Figure 13 includes the relationship between the force and the displacement at mid-span, obtained experimentally and with the computational code. The behaviour of the reference beams was captured quite well. For beams of series S3 and S4 the numerical model predicted an ultimate load a little bit lower the experimental one. This can be associated to the fact that it was not sure that the ϕ8 steel bars tested were the ones applied in these beams. It appears that the bars used in these beams have a yield stress higher than the value assumed in the numerical simulation. Figure 14 represents the typical crack patterns, at the last converged load increment, for the reference beams. Only the cracks completely open are represented. This crack patterns is representative of beams failed by bending.

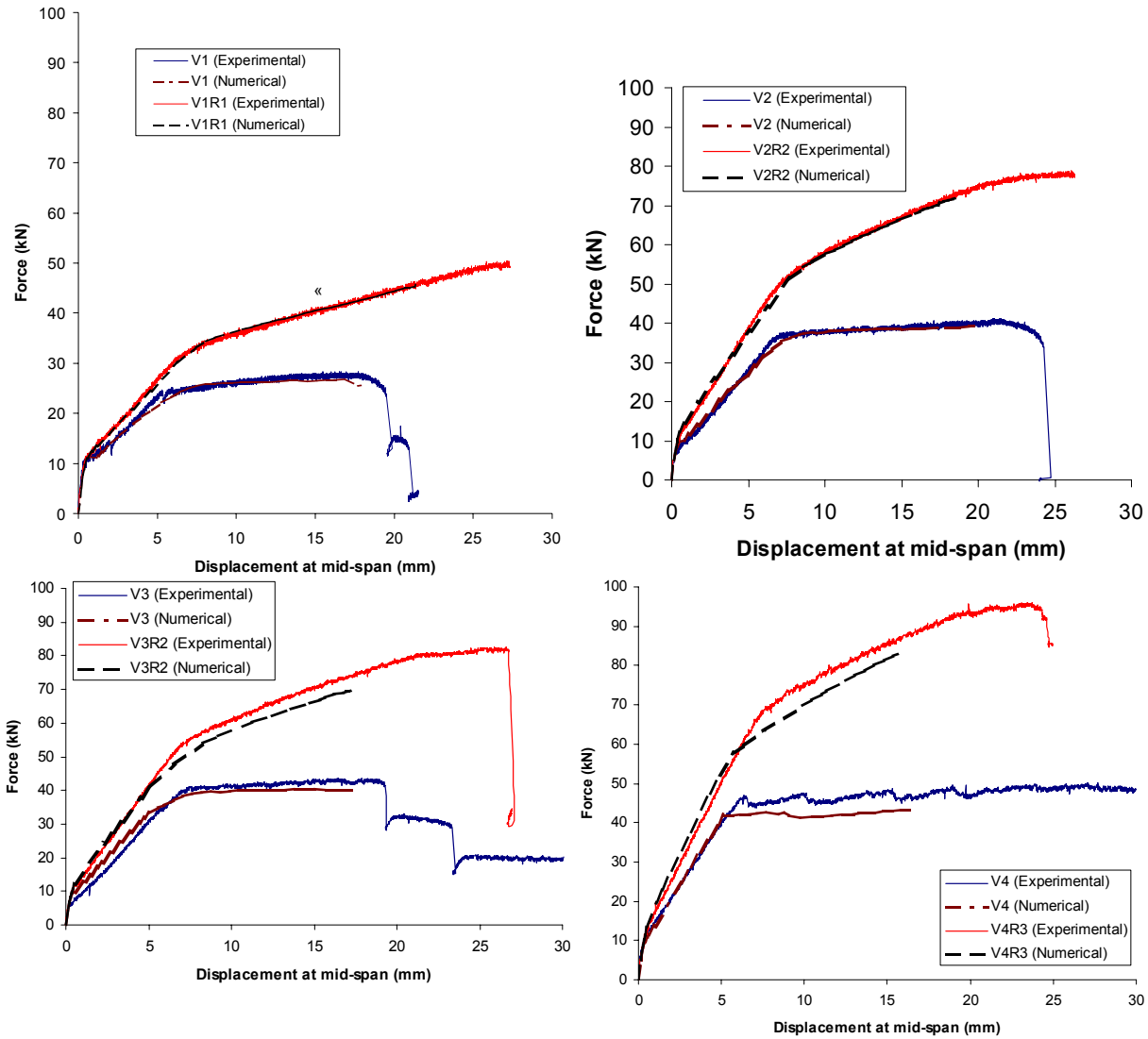

Figure 13. Experimental and numerical responses.

For the strengthened beams the model predicted a premature failure. After a certain moment the convergence was no more assured, even for very little load increments, crushing the concrete of several Gauss points due to high shear strains. This happens in the transition between the elements in stiffening and the elements in softening, at a level of about 60 mm, where the rupture surface was suddenly occurred in the experiments (see photos in Figure7). Figure 15 shows the typical crack patterns at the last converged load increment for the strengthened beams. It can be observed the development of horizontal and very inclined cracks, a first announcement of the aforementioned failure surface.

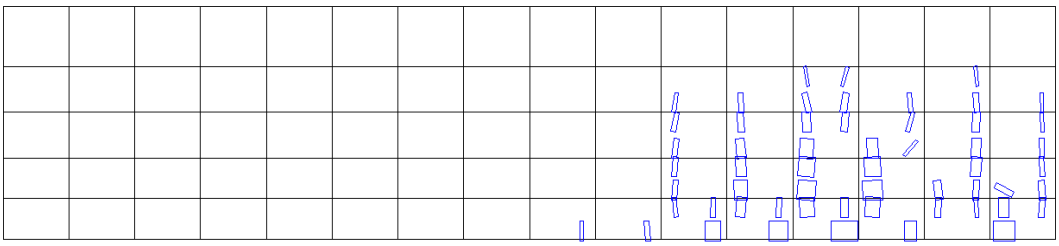

Figure 14. Typical crack patterns of reference beams at the last converged load increment. Only cracks completely open are represented (legend: a crack is represented by a rectangle with a width proportional to its normal crack strain).

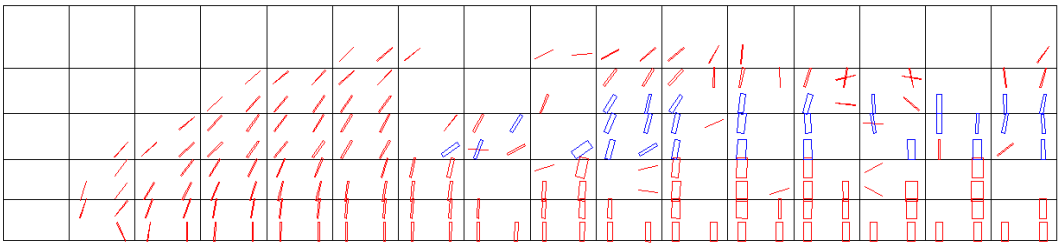

Figure 15. Typical crack patterns of strengthened beams in the last converged load increment. Only cracks in opening and completely open are represented: red colour => cracks in opening; blue colour => cracks completely open (see legend in Figure 13).

4 CONCLUSIONS

Four sets of concrete beams were strengthened with strips of CFRP laminates, using a technique different to the current ones. The amount of CFRP laminates was evaluated for doubling the ultimate load of the reference beams. This purpose was attained and the strengthening technique has revealed high efficacy, since the strain at CFRP laminates, at beam failure, was between 62% and 91% of the ultimate strain of CFRP laminates.

A computational code developed for material non-linear analysis of concrete reinforced with conventional steel bars was used for numerical simulation of the behaviour of the beams tested. Since the CFRP laminates were inserted into slits cut onto the concrete cover of the

beams, and fixed to concrete by epoxy adhesive, the slip between the CFRP laminates and the surrounded concrete is negligible. Therefore, in the model the CFRP laminates was considered perfectly bonded to concrete, like the conventional steel bars. The model has predicted, with enough accuracy, the response of the beams tested, but the failure of the strengthened beams was attained prematurely, giving ultimate loads 8.5% to 10% lesser the ones registered in the experiments.

5 - ACKNOWLEDGEMENTS

The authors of the present work wish to acknowledge the generous supports provided by the S&P®, Bettor MBT® Portugal (Engº Filipe Dourado), Secil, Cemacom (Dr. Paulo Nóvoas) and Solusel (Engº Fernandes). The second author aknowledges the grant provided by CAPES.

REFERENCES

[1] CEB-FIP. "Externally bonded FRP reinforcement for RC structures.", Technical report on the Design and use of externally bonded fibre reinforced polymer reinforcement (FRP EBR) for reinforced concrete structures, prepared by a working party of the Task Group 9.3 FRP (Fibre Reinforced Polymer) reinforcement for concrete structures, (2001).

[2] Juvandes, L.F.P., "Reforço e Reabilitação de Estruturas de Betão Armado usando Materiais Compósitos de "CFRP" ", PhD Thesis, Civil Eng. Dept., Faculty of Engineering, University of Porto, Portugal, (1999). (in Portuguese).

[3] – Dias, S. J. E., "Verificação experimental do reforço com CFRP de estruturas de betão à flexão", MSc Thesis, Dep. of Civil Engineer of Oporto University, (2001). (in Portuguese).

[4] – Barros, J.A.O., "Comportamento do betão reforçado com fibras - análise experimental e simulação numérica", PhD Thesis, Dep. of Civil Engineer of Oporto University, Dezembro de (1995). (in Portuguese).

[5] - ISO 527-5, "Plastics - Determination of tensile properties. Part 5: test conditions for unidirectional fibre-reinforced plastic composites", *International Standard ISO*: 9 pp. Genève, Switzerland, (1997).

[6] - ISO 527-3, "Plastics - Determination of tensile properties. Part 3: test conditions for films and sheets", *International Standard ISO*: 5 pp. Genève, Switzerland, (1997).

[7] - Barros, J.A.O., Figueiras, J.A. "Flexural behavior of steel fiber reinforced concrete: testing and modelling", Journal of Materials in Civil Engineering, ASCE, Vol. 11, Nº 4, pp 331-339, (1999).

[8] - Sena Cruz, J.M., Barros, J.A.O., Faria, R.M.C.M., "Assessing the embedded length of epoxy-bonded carbon laminates by pull-out bending tests", International Conference Composites in Construction, pp. 217-222, 10-12 October (2001).

[9] - Sena Cruz, J.M., Barros, J.A.O., "Bond behaviour of carbon laminate strips into concrete by pull-out bending tests", to be presented on the *Bond in Concrete – from research to standards*, Budapest, 20-22 November (2002).

[10] - Barros, J.A.O., Sena Cruz, J. "Fracture energy of steel fibre reinforced concrete", Journal of Mechanics of Composite Materials and Structures, Vol. 8, No. 1 pp.29-45, January-March (2001).

[11] – van Mier, J.G.M., "Fracture processes of concrete", CRC Press, ISBN 0-8493-9123-7, pp. 448, (1997).

[12] - Barros, J.A.O. "Analysis of concrete slabs supported on soil", IV Congreso Métodos Numéricos en Ingeniería, SEMNI, Sevilha, June (1999).

[13] - CEB-FIP Model Code Comite Euro-International du Beton, Bulletin d'Information nº 213/214, Ed. Thomas Telford, (1993).